DOI: 10.3901/CJME.2015.0305.023, available online at www.springerlink.com; www.cjmenet.com; www.cjme.com.cn

Rock Breaking Performance of a Pick Assisted by High-pressure Water Jet under Different Configuration Modes

LIU Songyong[1], LIU Xiaohui[1,*], CHEN Junfeng[2], and LIN Mingxing[3]

1 *School of Mechatronic Engineering, China University of Mining and Technology, Xuzhou 221116, China*
2 *Research Institute of Zhejiang University, Taizhou 318000, China*
3 *School of Mechanical Engineering, Shandong University, Jinan 250061, China*

Received June 30, 2014; revised March 3, 2015; accepted March 5, 2015

Abstract: In the process of rock breaking, the conical pick bears great cutting force and wear, as a result, high-pressure water jet technology is used to assist with cutting. However, the effect of the water jet position has not been studied for rock breaking using a pick. Therefore, the models of rock breaking with different configuration modes of the water jet are established based on SPH combined with FEM. The effect of the water jet pressure, distance between the jet and the pick bit, and cutting depth on the rock breaking performance as well as a comparison of the tension and compression stress are studied via simulation; the simulation results are verified by experiments. The numerical and experimental results indicate that the decrease in the rates of the pick force obviously increases from 25 MPa to 40 MPa, but slowly after 40 MPa, and the optimal distance between the jet and the pick bit is 2 mm under the JFP and JSP modes. The JCP mode is proved the best, followed by the modes of JRP and JFP, and the worst mode is JSP. The decrease in the rates of the pick force of the JCP, JRP, JFP, and JSP modes are up to 30.96%, 28.96%, 33.46%, 28.17%, and 25.42%, respectively, in experiment. Moreover, the JSP mode can be regarded as a special JFP model when the distance between the pick-tip and the jet impact point is 0 mm. This paper has a dominant capability in introducing new numerical and experimental method for the study of rock breaking assisted by water jet and electing the best water jet position from four different configuration modes.

Keywords: conical pick, high pressure water jet, rock breaking, SPH

1 Introduction

Conical picks are essential cutting tools that are widely used in engineering machinery. The pick that directly impacts rocks is in a harsh cutting environment. The low cutting efficiency and high cost of picks arise because the conical picks bear a great amount of the cutting force and wear quickly in the process of hard rock breaking[1]. To solve these problems, a great deal of research was performed by both scholars and engineers. One method that was presented involves changing the pick material and modifying the pick structural parameters. Carburization was performed on a 30CrMnMo alloy to synthesize a new cutting pick material with improved mechanical properties and high wear resistance[2]. Focusing on the structural characteristics of the cutting pick body and the material properties of 42CrMo high-strength steel, the power balance principle was used to obtain an approximation of the deforming force, and an approximate calculation formula of the warm extrusion force for the cutting pick body was derived. The result indicated that the method can refine the microstructure grain and improve the material performance[3–4]. The composite material WpC of a pick was studied to improve the hardness of the cutter tooth material[5]. Different pick structures were investigated to obtain the optimal structure; the results indicated that the pick structure had a great influence on rock breaking[6–8].

However, the methods described above are not effective for decreasing the cutting force and improving the cutting efficiency of picks. Picks are still easy to wear, resulting in a large consumption of picks and low economic benefits during rock breaking. Thus, foreign scholars proposed a new method, rock breaking via a conical pick assisted by a high-pressure water jet[9]. There are two main types of rock fragmentation via a water-jet assisted pick, the cutting effect and extrusion effect, as shown in Fig. 1. From Fig. 1(a), the rock is initially cut by the water-jet, which results in a certain depth of slotting and the formation of a free-surface on the rock surface, followed by fragmentation via machine tools. This approach can improve the rock fragmentation efficiency and reduce the cutting force of the machine tools. From Fig. 1(b), the water jet acted via an extrusion effect. In this approach, under the action of cutting via machine tools, cracks are generated, which

* Corresponding author. E-mail: TB13050011@163.com
Supported by National Natural Science Foundation of China(Grant No. 51375478), the Fundamental Research Funds for the Central Universities, China(Grant No. 2014ZDPY12), and the Priority Academic Program Development of Jiangsu High Education Institute of China

extend and propagate via the water-jet, leading to rock breaking.

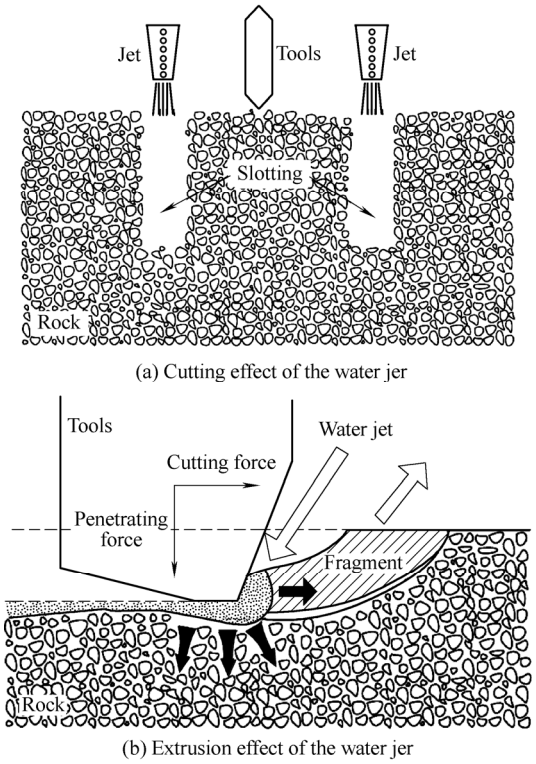

Fig. 1 Different rock fragmentation types via a pick assisted by water jet

The mechanism of rock breaking via a pick assisted by a high-pressure water jet was studied and found to be divided into three processes[10]: 1) the hydraulic erosion process, when the water jet erodes the rock breaking zone; 2) the hydraulic fracturing process, when the expansion of micro cracks is accelerated by a water jet; and 3) the pore pressure process, when a pressurized water jet produces expansion, thus accelerating crack initiation and propagation. A research program at the Colorado School of Mines investigated the application of low-to-moderate pressure water jets to assist the cutting performance of drag-type cutter bits commonly used on coal mine cutting machinery. The results indicated that a water jet directed to impinge the rock in the immediate vicinity of the cutter tip can provide significant benefits in terms of reduced cutting forces, prolonged bit life, and reduced airborne dust as well as a reduced tendency for sparking during cutting[11].

The research on this method has shown that rock breaking via a pick assisted by a high-pressure water jet can reduce the load of the pick and improve the cutting efficiency of the pick. Thus, much research has been conducted on rock breaking via a pick assisted by a high-pressure water jet.

LI X B, et al[12], performed experiments on the performance of PDC cutters resisting different combined loads of static thrust, impact, cutting and a water jet on Missouri red granite and Halston limestone to verify the feasibility and efficiency of drilling assisted by a water jet in hard rock when the water jet pressure was 42 MPa–49 MPa; the results indicated that the combined mode of cutting-impact was effective in hard rock. KOTWICA K[13] presented the results for the investigations conducted on a test stand involving cutting artificial samples of rock with an ultimate compressive strength of up to 105 MPa, both with and without the high-pressure water jet supply. CICCU R, et al[14], conducted an experiment on the mining performance of a PDC tool assisted by a 150 MPa water jet. The results indicated that the water jet helped to improve the speed of mining and reduce tool wear; in addition, the mining depth of the trench was found to be increased by 80%. OZCELIK Y, et al[15–16], focused on the stone surface treatment using water jets and concluded that the application of water jets to the surface treatment enabled the development of a surface with the required roughness while preserving the aesthetic appearance of the stone. The experiments were also conducted using a pure water jet on Italian granite samples to determine the effects of different operational parameters (traverse velocity, standoff distance and pump pressure) on the performance parameters (cutting depth and cutting width)[17]. YANG, et al[18], studied the wear characteristics of the cemented carbide blades when drilling limestone with a water jet and concluded that the wear rates decrease with the increase of the nozzle diameter in the drill bit. LU Y, et al[19], conducted experiments using a water jet and compared the results with the results of the conventional technique; the comparison indicated that with the assistance of an abrasive water jet, the drilling depth increased by approximately 63%, while the thrust force and torque reduced by approximately 15% and 20%, respectively. PENG G Y, et al[20], discussed the properties of existing cavitations models and introduced a compressible mixture flow method for the numerical simulation of high-speed water jets accompanied by intensive cavitations. DEHKHODA S, et al[21–22], investigated the capacity of pulsed water jets for creating the internal breakdown and relative contributions of the pulse length and pulsation frequency on the surface and sub-surface damage caused by a pulsed water-jet on the rock targets. With the development of the water jet technique, a new method, called the abrasive water jet (AWJ) assisted method, was developed for use in hard rock mechanical cutting and drilling[23]. AYDIN G, et al[24], investigated the significant rock properties affecting the recycling of abrasives in the AWJ cutting of granites. CICCU R, et al[25], studied disc cutters assisted by means of high-velocity jets of water, with the aim of increasing the excavation rate while improving the working conditions (with particular reference to wear). The results indicated that a higher removal rate was achieved due to the weakening action of a jet directed on one side of the disc, causing deeper penetration. LIU S Y, et al[26–27], established the damage models of rock breaking with a conical pick assisted by a water jet based on SPH combined with the finite element method, the results of which were compared

with experiments. SONG D Z, et al[28], analysed the possibility and reasonableness of water jet cutting technology(WJCT) application to rock burst relief and prevention, simulated the distributive characteristics of stress and energy fields suffered by hard coal roadway wall rock and the internal relationships of the fields to the instability, and conducted field tests of WJCT using electromagnetic radiation(EMR) measurement technology.

The above works provided reference materials for our research; however, very little machinery equipment for rock breaking via a pick assisted by a water jet has been put into production. Some researchers have conducted semi-industrial and industrial tests, but such studies were ultimately discontinued. The reasons for this lack of progress were that the position between the water jet and the bit was not appropriate; as a result, rock breaking via a pick assisted by a water jet was not effective. The research paid more attention to the rock breaking using a pick assisted by a water jet placed in front of the pick(JFP) and behind the pick(JRP), as shown in Fig. 2(a) and Fig. 2(b), respectively. A jet through the centre of the pick(JCP) and a jet placed at the side of the pick(JSP), as shown in Fig. 2(c) and Fig. 2(d), respectively, have received little attention.

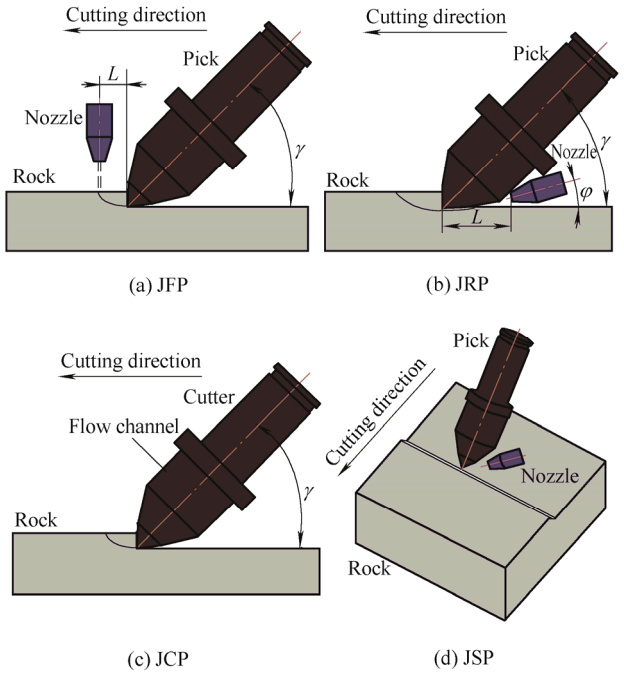

Fig. 2. Model of rock breaking via a pick assisted by water jet

It is necessary to study the rock breaking performance and configuration mode of a pick assisted with a high-pressure water jet to solve the difficult problem of hard rock excavation. The method of SPH combined with the finite element method was proposed in this paper, and the rock breaking models of a pick assisted by a water jet were built for four modes(JCP, JFP, JSP, and JRP). The dynamic process of rock breaking and the force of the pick were analysed in the four configuration modes. In addition, the effects of the water jet pressure, the distance between the jet and the pick tip, and the cutting depth were studied. Moreover, numerical simulations and experiments were conducted to determine the optimal configuration mode. This research is aimed at improving the efficiency of rock breaking, slowing down pick wear, and providing a reference for further research studies on rock breaking via a conical pick assisted by a water jet.

2 Numerical Model

2.1 SPH method

SPH is a new class of mesh-free method that has been developed to efficiently solve large deformation problems by constructing an approximation completely based on the nodes instead of the meshes. SPH was first applied to solve astrophysical problems and has been extensively applied in various fields, such as fluid dynamics, molecular dynamics, and solid mechanics. Because of its mesh-free features, SPH can be applied to solve discontinuous problems through continuum mechanics. SPH was successfully demonstrated to be applicable for the simulation of fluid impacts[29].

The SPH method is a completely mesh-free technique, enabling the modelling of fluid particle trajectories accordingly to the Navier–Stokes equations and is written using SPH formalism based on the theory of interpolation integrals, which uses interpolation kernels. The Lagrangian approach of the SPH method consists of following the fluid particles in a determined time interval to obtain its trajectories, velocities and pressures as a function of the initial position and time[30].

The theoretical basis of SPH is interpolation theory. By introducing an interpolation function(kernel function W) that provides the 'kernel estimate' of the field variables at a point, the properties of each particle are evaluated via the integrals or the sums over the values of its neighbouring particles. Here, we consider a problem domain Ω that is discretised by a group of particles, as shown in Fig. 3.

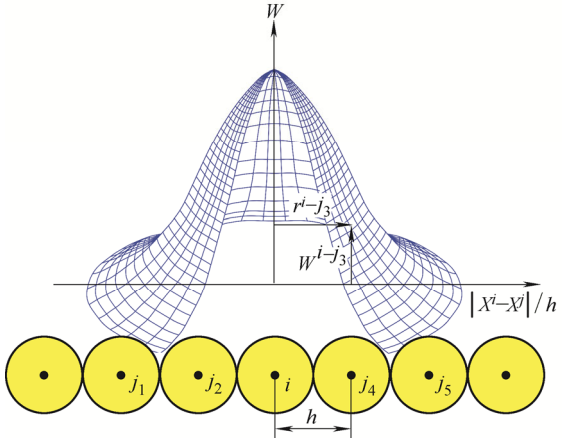

Fig. 3. Kernel function for theoretical basis of SPH

Assuming that there is a compact supporting domain with a radius of h, the approximations of a function $f(x)$

and its differential form $<f(x)>$ at point i can be expressed by the discretised particles as follows[31]:

$$<f(x)>_{x=x_i}=\sum_{j=1}^{N}\frac{m_i}{\rho_j}f(x)\bullet W_{x_i}(x_i-x_j,h), \tag{1}$$

$$<\nabla f(x)>_{x=x_i}=-\sum_{j=1}^{N}\frac{m_j}{\rho_j}\left[f(x_i)-f(x_j)\right]\bullet\nabla W_{x_i}(x_i-x_j,h), \tag{2}$$

where the summation is over all of the particles with a total number of N, including particle i within the supporting domain of the given particle i; the label j are the influenced particles that are the neighbouring particles of particle i; m_j is the mass of particle j; h is the smoothing length, which defines the supporting domain of the particle; and $W_{x_i}(x_i-x_j,h)$ is the smoothing kernel function.

To build the numerical models of rock breaking using a pick assisted by a water jet, the model of the rock was established using the finite element method; the model of the water jet was established using the SPH method, in which the water jet was discretised into SPH particles. If the coordinate of the particle α was x_i at the initial time, then it would be x_j at time t. Thus, the position of particle α is a function of the initial coordinate x_i, namely, $x_j=x_j(x_i,t)$. In hydromechanics, the following equations are often used to describe the motion and status of the fluid when the hydrodynamics problems are solved using the SPH method[32–34].

The position equation of the particle is

$$\frac{\mathrm{d}x_i}{\mathrm{d}t}=v_i. \tag{3}$$

The mass conservation equation of the particle is

$$\frac{\mathrm{d}\rho}{\mathrm{d}t}(x_i)=\sum_{j-1}^{N}m_j\left[v(x_j)-v(x_i)\right]\bullet\nabla_i W_{ij}. \tag{4}$$

The momentum conservation equation of the particle is

$$\frac{\mathrm{d}v}{\mathrm{d}t}(x_i)=\left[\frac{\sigma^{\alpha\beta}(x_j)}{\rho_i^2}-\frac{\sigma^{\alpha\beta}(x_i)}{\rho_j^2}\right]\bullet W_{ij,\beta}. \tag{5}$$

The energy conservation equation of the particle is

$$\frac{\mathrm{d}E}{\mathrm{d}t}(x_i)=\sum_{j-1}^{N}m_j\left[v(x_j)-v(x_i)\right]\left[\frac{\sigma^{\alpha\beta}(x_j)}{\rho_i^2}+\frac{1}{2}\Pi_{ij}\right]\bullet W_{ij,\beta}+H_i, \tag{6}$$

where $\rho(x_i)$ is the density of particle i; m_j is the mass of the particle j (kg); $\sigma^{\alpha\beta}$ is the stress tensor (Pa); $v(x_i)$ is the velocity of particle i (m/s); $E(x_i)$ is the internal energy per unit mass of particle i (J); Π is the artificial viscosity force (N); H is the artificial heat flux (J/s); and W is the kernel function of the particle.

2.2 Failure criterion of the rock

Rock breaking can be expressed by the rock failure criterion. In LS-DYNA, the nonlinear material Drucker_Prager[35] was used to imitate the rock based on the following algebraic expression:

$$\beta I_1+\sqrt{J_2}-\kappa=0, \tag{7}$$

where J_2 is invariant of the stress deviator, κ and β are the correlative coefficients.

Parameters κ and β in Eq. (7) are determined according to the Eq. (8) and Eq. (9):

$$\beta=\frac{\sqrt{3}\sin\varphi}{3\sqrt{3}+\sin^2\varphi}=\frac{\tan\varphi}{\sqrt{9+12\tan^2\varphi}}, \tag{8}$$

$$\kappa=\frac{\sqrt{3}c\cos\varphi}{3\sqrt{3}+\cos^2\varphi}=\frac{3c}{\sqrt{9+12\tan^2\varphi}}, \tag{9}$$

where c is the cohesive force, and φ is the internal friction angle of rock.

To realize the failure criterion of the rock, the parameters of the rock were set by adding the Erosion Keyword "Mat_Add_Erosion" in LS-DYNA.

2.3 Finite element model

The parameters of the rock and the conical pick in the numerical models are presented in Table 1.

Table 1. Mechanical parameters of the rock and pick

Material	Density ρ/(kg • m^{-3})	Elastic modulus E/GPa	Poisson ratio v	Compressive strength σ/MPa
Rock	2456	29.57	0.26	37.48
Pick	14 600	600	0.22	

To compare the efficiencies of the four modes(JCP, JFP, JBP, and JSP), simulations were performed under the conditions of different cutting depths(5 mm, 10 mm, 15 mm, and 20 mm). The size of the rock was 580 mm×400 mm×200 mm, and the material of the rock was Drucker_Prager. The cutting speed of the pick was 2 m/min in the simulations. The simulation models are shown in Fig. 4.

The theoretical speed of the high pressure water jet is

$$v=44.67\sqrt{P}. \tag{10}$$

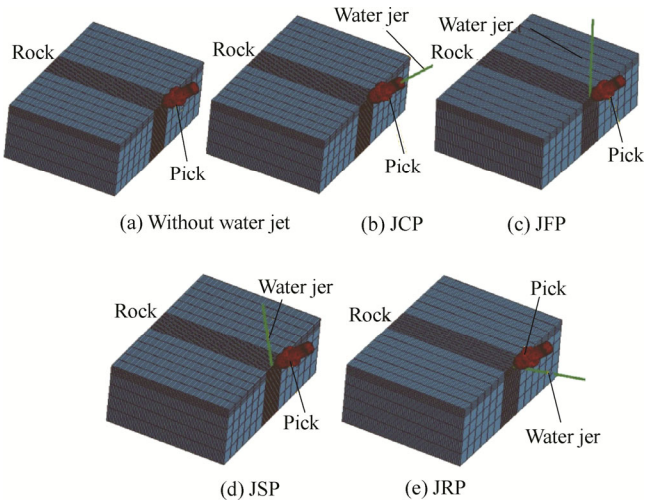

Fig. 4. Numerical models of the different configuration modes

In the simulations, only the jet velocity can be defined in LS-DYNA; according to Eq. (10), when converted to the jet impact velocity, the jet pressure was set to 25 MPa, 40 MPa, 50 MPa, and 60 MPa; the radius r of the water jet was 1 mm; and the advance speed v_1 of the water jet was 2 m/min. In the LS-DYNA code, the MAT-NULL has no shear stiffness, and the GRUNEISEN equation of state (EOS) for the pressure response can be used to describe the behaviour of water: the density is 1000 kg/m^3, the dynamic viscosity is 0.001 Pa • s, and the Poisson ratio is 0.5. Additionally, the EOS_GRUNEISEN is given by Eq. (11) to describe the relationship between pressure and volumetric strain:

$$Q=\frac{\rho c^2\mu\left[1+\left(1-\frac{\gamma_0}{2}\right)\mu-\frac{\alpha}{2}\mu^2\right]}{\left[1-(S_1-1)\mu-S_2\frac{\mu^2}{\mu+1}-S_3\frac{\mu^3}{(\mu+1)^2}\right]^2}+(\gamma_0+\alpha\mu)E, \tag{11}$$

where E, the internal energy of unit volume, is set to 2.86e^{-6} J; C, the intercept of the curve μ_s–μ_p (relationship between wave velocity and particle velocity), is set to 1647; S_1, S_2 and S_3, the slopes of the curve μ_s–μ_p, are set to 1.921, –0.096 and 0, respectively; γ_0, the EOS_ GRUNEISEN coefficient, is set to 0.35; α, the correction coefficient about the relationship between the EOS_ GRUNEISEN coefficient and volume, is set to 0. The main research parameters were shown in Table 2.

Table 2. Simulation parameters of water jet and pick

Parameter	Value				
Jet pressure p/MPa	0	25	40	50	60
Distance between pick-tip and jet impact point l/mm	2	5	10	15	
Cutting depth d/mm	5	10	15	20	
Cutting tool	JCP	JFP	JSP	JRP	

3 Numerical Results

3.1 Influence of the jet pressure and the cutting depth

To study the rock breaking effect assisted with a high-pressure water jet under different configuration modes, a contrastive analysis of the force distribution of a pick was conducted. When the pressure of water jet was 25 MPa, 40 MPa, 50 MPa, and 60 MPa and the cutting depth was 10 mm, the force of the JCP and a pick are shown in Fig. 5.

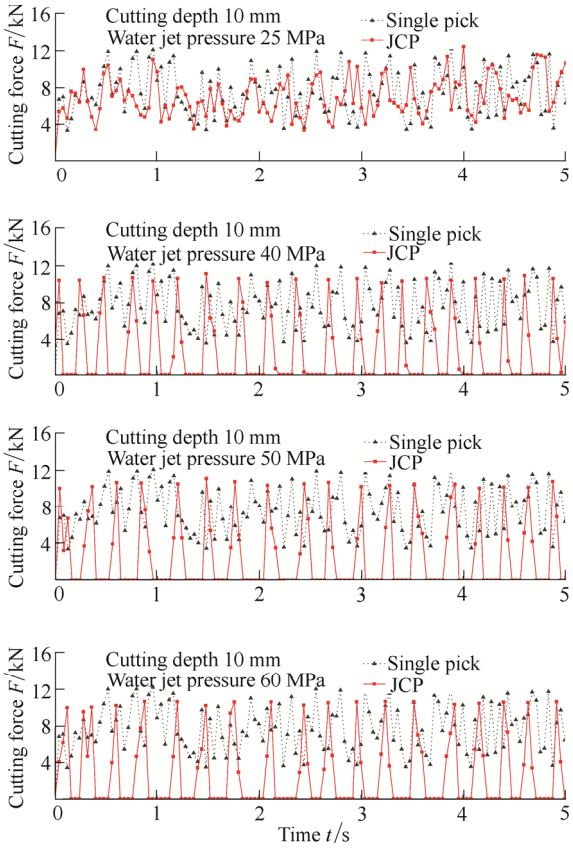

Fig. 5. Comparison of cutting force of a JCP and a single pick

Fig. 5 shows that the assistance of the water jet is not effective for rock breaking when the pressure of the water jet is 25 MPa, but it becomes effective when the pressure of the water jet exceeds 25 MPa(i.e., 40 MPa, 50 MPa, and 60 MPa in this study). Compared with a pick, the force curve of the JCP moves down and the peak force declines. Initially, the cutting force of a pick increases rapidly due to the elastic deformation occurring on the rock surface. Next, the cutting force will decrease to the minimum until the rock unit reaches fracture strength.

The probability of decreasing the cutting force to zero reduces with the water jet pressure in the simulations. The reason for this observation is that the energy of the cracks gained in the rock breaking process is uneven, which will lead to the remnant of a rock ridge on the bottom of the grooving. The remaining rock ridge is low when the water jet pressure is small and the required cutting force is small, that is, the probability of the cutting force dropping to zero is high. Conversely, when the required cutting force is high,

the probability of the cutting force dropping to zero is low.

The average force extracted from the force curve was used to quantitatively analyse the simulation results. When the distance between the jet and the pick-tip was 5 mm, the rates of the pick force under different water jet pressures(25 MPa, 40 MPa, 50 MPa and 60 MPa) and different cutting depths(5 mm, 10 mm, 15 mm and 20 mm) decreased, as shown in Fig. 6.

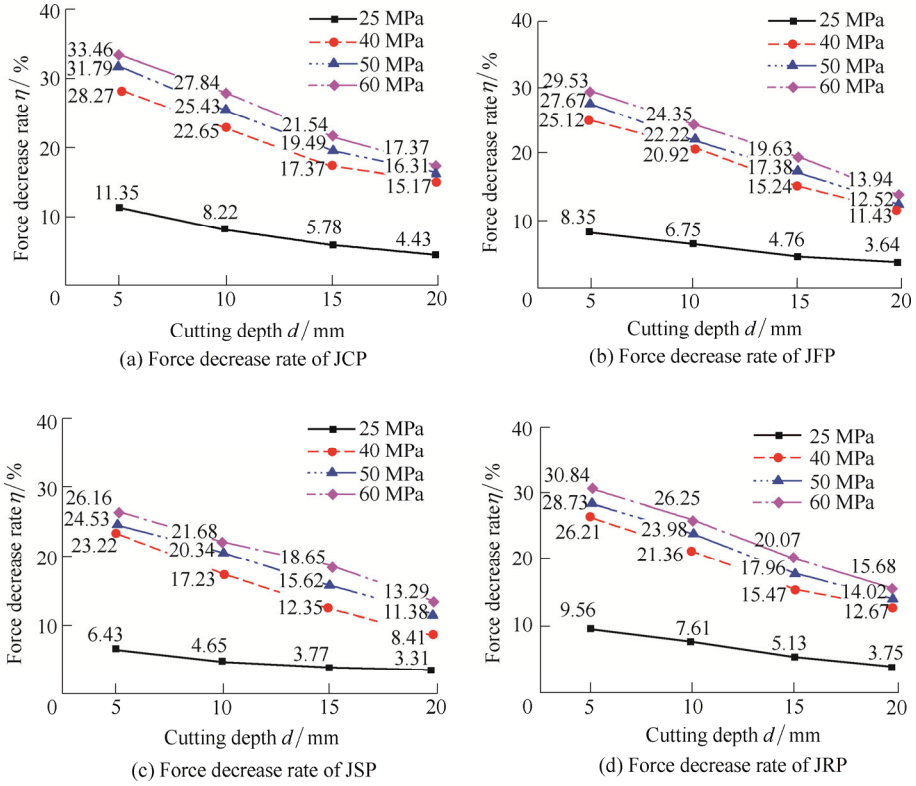

Fig. 6. Force decrease rate of the different configuration modes in simulation

Fig. 6 shows that the rates of the decrease of the pick force increase with the pressure of the water jet. Because the energy loss of the water jet will be increased if the pressure of the water jet is raised, the impact and wedge action of the water jet are affected; as a result, the peak cutting force decreases.The rates of the decrease of the pick force increases over the pressure range of 25 MPa to 40 MPa, but slowly from 40 MPa to 60 MPa. The decreased rate of a pick force, such as the JCP, is 11.35%, 28.57%, 31.79% and 33.46% with the pressure of the water jet of 25 MPa, 40 MPa, 50 MPa and 60 MPa, respectively, when the cutting depth is 5 mm.

A specific critical point(rock compressive strength) was found for the effect of the water jet pressure on the pick force under different configuration modes. When the jet pressure is lower than the compressive strength of rock, the increase of the jet pressure has a small influence on the decrease rates of the pick force. In other words, the efficiency of rock breaking is improved with the assistance of a water jet when the pressure of the water jet is higher than the compressive strength of the rock. In addition, the rates of reduction of the pick force reduce with the increase of the cutting depth. The deeper the cutting depth is, the worse the effect of water jet is. The result indicates that the assistance effect of JCP is best, followed by JRP, while JSP is the worst.

The main reason for why the cutting force of the JCP model is minimized is that rock is easy to break via a pick assisted by a centre water jet. The better the breakage of rock, the fewer the number of obstacles for the pick advancing and the smaller the cutting force.

3.2 Influence of distance between jet impact point and pick-tip

3.2.1 JFP

The distance from impact point of the water jet to the pick tip is a critical factor in the combined effect of the water jet and the pick. The equivalent stress distribution of the rock is shown in Fig. 7 for distances of 2 mm, 5 mm, 10 mm, 15 mm when the jet pressure is 40 MPa and the cutting depth is 10 mm.

Fig. 7 indicates that stacking stress of the rock interior reaches its maximum when the distance between the water jet and the pick tip is 2 mm. In addition, rock breaking becomes easier. However, there are clear limits for the stress wave when the distance is too small. The scope of the stacking stress wave is too small to widely break the rock. When the distance reaches 5 mm, the scope of the stacking stress wave significantly increases, reaching a maximum

stress of 21.87 MPa. When the distance reaches 10 mm, the maximum valve of the superimposed stress wave decreases, but the red area greatly increases. When the distance is 15 mm, the stress wave is obviously greatly limited due the excessively large distances. The rapid attenuation causes the poor effect of stress wave superposition and rock breaking. As a result, to break rock more easily and effectively, the optimal distance between the impact point of the water jet and the pick tip is 2 mm according to the simulation results. However, in theory, the scope of the stacking stress wave is wider and the pieces of rock breaking are larger when the distance is 5 mm.

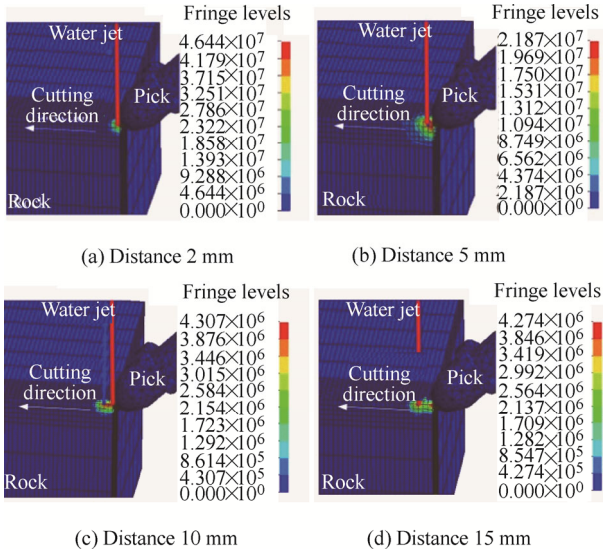

(a) Distance 2 mm (b) Distance 5 mm

(c) Distance 10 mm (d) Distance 15 mm

Fig. 7. Equivalent stress of different distance between the water jet impact point and pick-bit

3.2.2 JSP

The equivalent stress distribution of the numerical model under the same condition as the JSP is shown in Fig. 8.

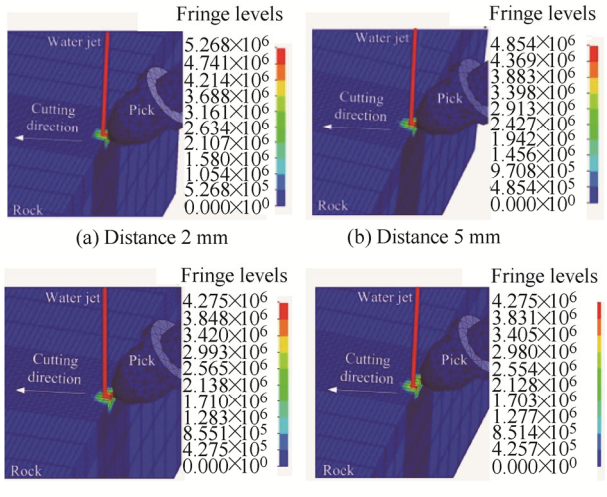

(a) Distance 2 mm (b) Distance 5 mm

(c) Distance 10 mm (d) Distance 15 mm

Fig. 8. Equivalent stress of different distance between the water jet impact points and pick-bit

Fig. 8 indicates that the farther the distance between the impact point of the water jet and the pick tip, the smaller the maximum stress of the rock. The maximum stress of the rock under the combination of a pick with a water jet is 5.268 MPa, 4.854 MPa, 4.275 MPa, and 4.257 MPa for the distance of 2 mm, 5 mm, 10 mm, and 15 mm, respectively. When the distance is greater than 15 mm, the effects of stress from the water jet and the cutting stress are mostly separated, which leads to a poor stress superposition effect. In contrast, a preferable crushing effect is observed for the distance of 2 mm.

3.3 Comparison of tension and compression stress

The tension and compression stress distribution at 0.04 s under a pick, the JCP, the JFP, the JSP and the JRP are shown in Fig. 9. To clearly observe the stress distribution, the SPH jet was hidden in the post-processing and the rock was divided along cutting direction.

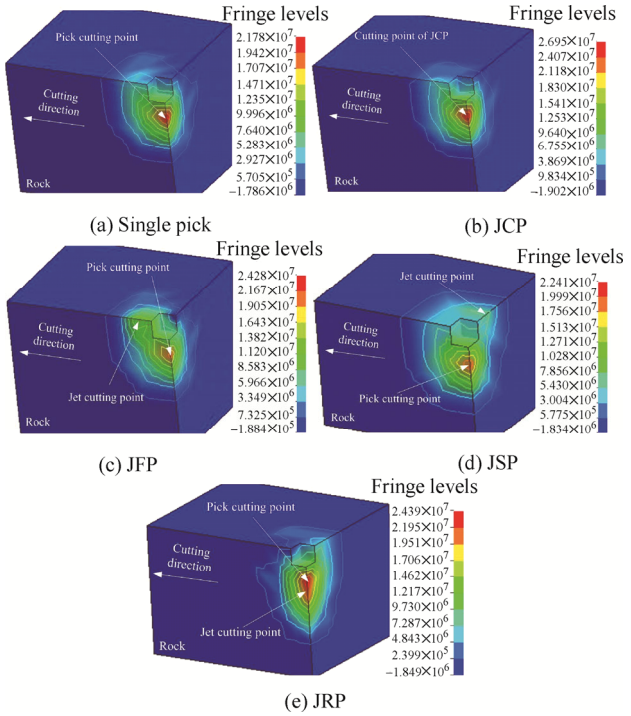

(a) Single pick (b) JCP

(c) JFP (d) JSP

(e) JRP

Fig. 9. Comparisons of the rock compressive stress

Fig. 9 shows that the maximum compression stress of the pick, JCP, JFP, JSP and JRP is 21.78 MPa, 26.95 MPa, 24.28 MPa, 22.41 MPa, and 24.39 MPa, respectively. The rock breaking effect of the JCP is the best, based on the analysis of the crushing destruction. The maximum tension stress of the rock breaking of the pick, JCP, JFP, JSP, and JRP is 1.786 MPa, 1.902 MPa, 1.884 MPa, 1.834 MPa, and 1.849 MPa, respectively. The test rock specimen is taken as a brittle material, the tension stress of which is far lower than the compression stress, that is, tensile fracture is much more apt to occur in rock specimen. Thus, considering tensile fracture and crushing fracture, the effect of the rock breaking of the JCP is the best, followed by the JRP, the JFP and the JSP in sequence.

Moreover, the compression stress of the jet impact point and pick impact point cannot be superposed effectively

when the action point of the water jet and the pick were not the same. Fig. 9(b) shows that the rock was compressed at the beginning of rock cutting under the JCP. The compression stress in the impact centre is highest, with a maximum of 26.95 MPa. The compression stress decreases and gradually turns into tension stress with the increase of the radial distance. The maximum tension stress appears around the jet impact point, with a value of 1.902 MPa. The tension crack forms at the edge of the impact centre.

4 Experiment Research

To obtain the optimal pick and jet arrangement and verify the correctness of the numerical models, experiments of rock breaking with the assistance of a water jet for different configuration modes(JCP, JFP, JSP, JRP) were performed. The cutting forces of different pick and jet arrangements were measured and recorded. The test bed for rock breaking with the assistance of a high-pressure water jet is shown in Fig. 10.

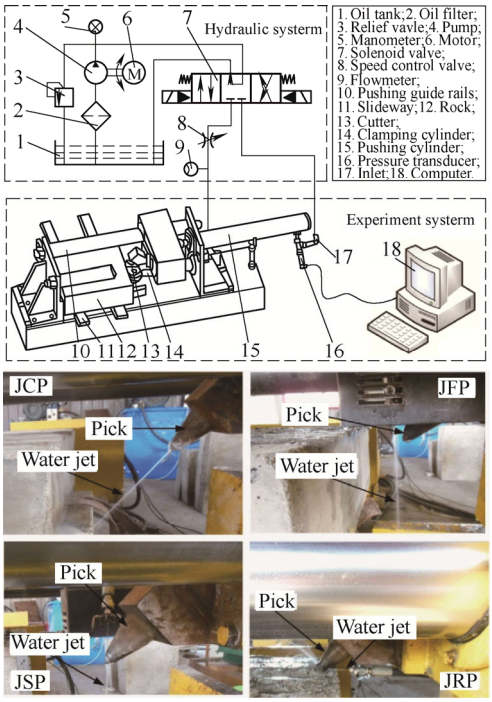

Fig. 10. Rock & coal cutting test-bed and different configuration modes

Fig. 10 shows that the rock sample was clamped on the test bench by clamping cylinder 14. Rock slide 11 can reduce the friction between the rock samples and the test platform, which can conveniently load and move the rock. Pushing cylinder 15 can realize a linear reciprocated cutting action propelling along rail 10. The cutting depth can be regulated by changing the thickness of the steel plate under the rock samples. The propulsion force of the pick can be measured using pressure sensor 16 JNBP-10.

The experimental parameters used, which are similar to those of the simulation, are presented in Table 3 for the rock sample size of 580 mm×400 mm×200 mm.

Table 3. Experimental parameters

Parameter	Value				
Jet pressure p/MPa	0	25	40	50	60
Distance between pick-tip and jet impact point l/mm	2	5	10	15	
Cutting depth d/mm	5	10	15	20	
Cutting tool	JCP	JFP	JSP	JRP	

The pressure sensor measured different pressures of the centre jet and bit load when the cutting depth was 5 mm, as shown in Fig. 11.

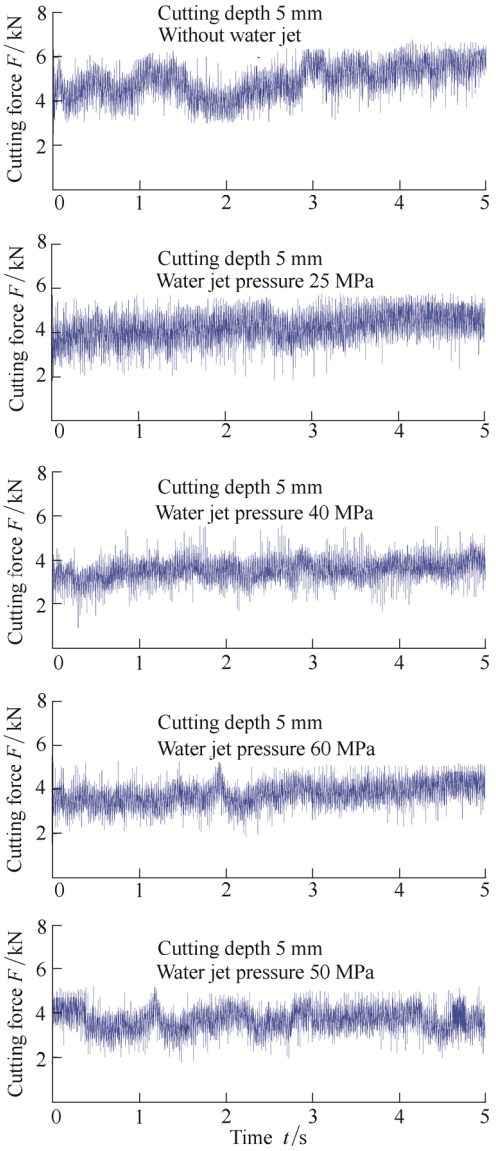

Fig. 11. Cutting force of rock breaking under different pressures at a cutting depth of 5 mm

Fig. 11 shows that the force wave curve decreases significantly with the increase of the water pressure and that the stress decreases with the water jet pressure when the cutting depth is 5 mm. In addition, the force was observed to greatly fluctuate without the water jet, while the stress wave slowly changed with the water jet.

To illustrate the rock breaking effect of the water jet

more clearly, the average value and the rate of decrease of the pick load under the different configuration modes were calculated according to the stress wave, as shown in Fig. 12.

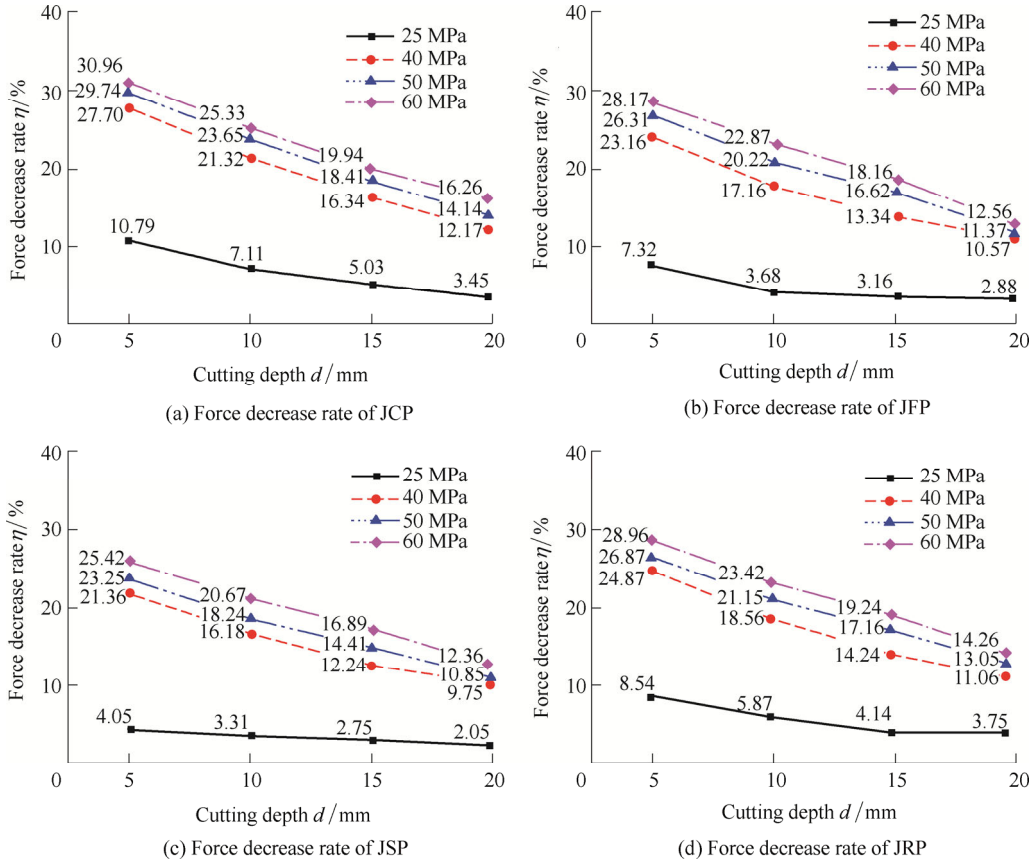

(a) Force decrease rate of JCP

(b) Force decrease rate of JFP

(c) Force decrease rate of JSP

(d) Force decrease rate of JRP

Fig. 12. Force decrease rate of different configuration mode in experiments

From Fig. 12, the rate of decrease of the cutting force increases with the water jet pressure. When the water jet pressure is lower than the compressive strength of the rock, the rock breaking effect assisted by the water jet is poor; otherwise, the rock breaking effect assisted by the jet is high. With the increase of the cutting depth, the rate of decrease of the force due to the jet decreases, and the larger the cutting depth, the worse the rock breaking effect assisted by the jet. From the rate of the force decrease, the rate of decrease of the cutting force of the JCP has a maximum of 30.96%, followed by the JRP at 28.96%, the JFP at 28.17%, and the JSP at 25.42% under the same conditions. The simulation results are consistent with the numerical results, thus verifying the correctness of the numerical models.

Compared with the numerical simulation results, the force decease rates in the experiment are slightly less than those of the results of the numerical simulation. From the analysis, some friction exists between the propulsion device and the guide rail, and internal friction is found in the cylinder in the experimental cutting process, which leads to the increase of the cutting force.

The cutting depth was set to 10 mm, and the distance between the pick tip and the jet impact point was set to 2 mm, 5 mm, 10 mm, and 15 mm. The force decrease rate is shown in Fig. 13 for different distances between the pick tip and the jet impact point for water jet pressures of 25 MPa, 40 MPa, 50 MPa, and 60 MPa.

From Fig. 13, the decrease rate of cutting force decreases with the increase of the distance between the pick tip and the jet impact point. Within the scope of this study, the distance between the pick tip and the jet impact point should be as small as possible; thus, the best distance is 2 mm. Comparing the JFP with the JSP, the cutting force decrease rate of the JFP is flat, while that of the JSP decreases greatly. Moreover, there is little effect of the distance between pick tip and the jet impact point on the JFP, while a great effect is found on the JSP. Analysis of the data indicates that the water jet of the JFP can still form grooves with the increase of the distance between the pick tip and the jet impact point in the cutting direction, but the JSP cannot. Thus, when the jet was arranged in front of the pick, the change rate of the cutting force decreased slightly and the overall trend variation was minor.

However, for the JSP, the grooves were not in the cutting direction; thus, the jet assisted effect decreased with increasing distance, which can be inferred from Fig. 14.

Fig. 14 shows that the farther the distance between the pick tip and the jet impact point, the worse the effect of the water jet for rock breaking, which means that there is no combined effect of the jet and the pick for rock breaking. Therefore, when the distance is 15 mm, the groove formed

by the pick is completely separate from that formed by the jet. When the distance is 2 mm, the two grooves formed by the pick and the jet are combined. When the distance is 5 mm, the combined groove is observed to be greater than that for the distance of 2 mm. Thus, the optimal distance is approximately 2-5 mm. From the analysis of the decrease of the rate of the pick force, it was at a maximum when the distance was 2 mm, which was accepted as the best value.

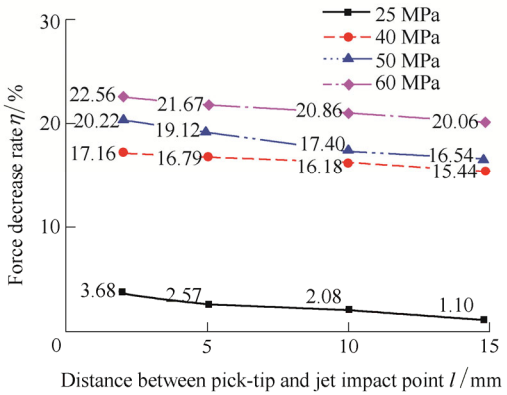

(a) Force decrease rate of JFP in different distance

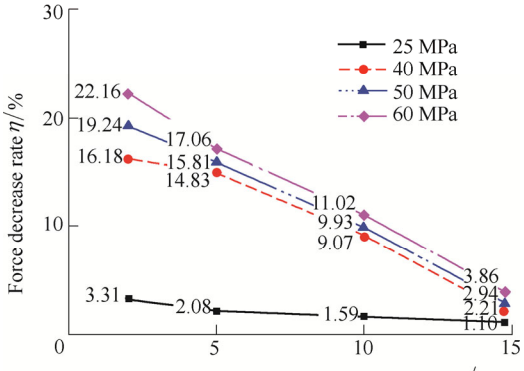

(b) Force decrease rate of JSP in different distance

Fig. 13 Force decrease rate in different distance between pick bit and jet impact point

Moreover, the JSP model can be regarded as a special JFP model when the distance between the pick-tip and the jet impact point is 0. It can be speculated from the analysis that the longer the distance, the less effective the water jet.

5 Conclusions

(1) The rates of decrease of the pick force increase in the range from 25 MPa to 40 MPa, but only slowly increase in the range from 40 MPa to 60 MPa; the distance between the pick tip and the jet impact point is found to be optimal at 2 mm for the JFP and JSP in the rock breaking process.

(2) The JCP is proved the best to decreasing cutting force, followed by the JRP and the JFP, and the worst is the JSP. For a cutting depth of 5 mm and for a water jet pressure of 60 MPa, the rate of decrease of the pick force of the pick, the JCP, the JRP, the JFP and the JSP are 33.46%, 30.84%, 33.46%, 29.53%, and 26.16%, respectively, in the simulations, while 30.96%, 28.96%, 33.46%, 28.17%, 25.42%, respectively, in experiments.

(3) The JSP model can be regarded as a special JFP model when the distance between the pick tip and the jet impact point is 0 mm. And the longer the distance between the pick tip and the jet is, the less effective the water jet is.

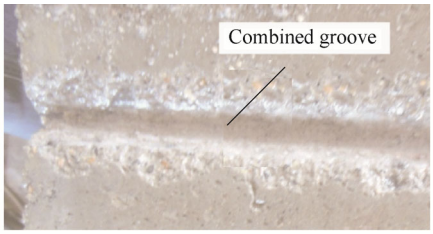

(a) Distace 2 mm

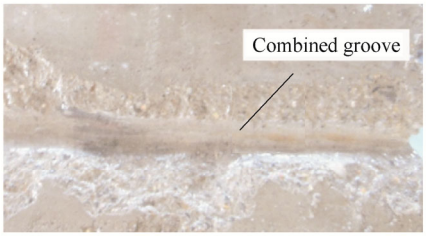

(b) Distance 5 mm

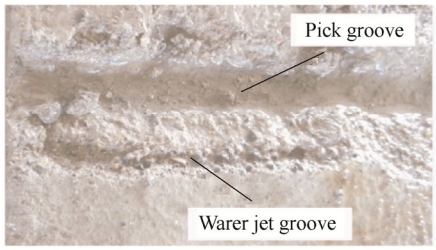

(c) Distance 10 mm

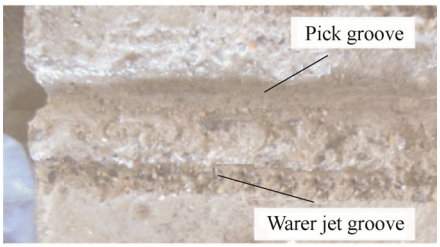

(d) Distance 15 mm

Fig.14 Grooves at different distance between the pick-tip and jet impact point

References

[1] LIU X H, LIU S Y, CUI X X, et al. Interference model of conical pick in cutting process[J]. *Journal of Vibroengineering*, 2014, 16(1): 115–128.

[2] LUO Y, ZHANG D K, WANG Q L, et al. Preparation and properties of a new cutting pick of coal shearers[J]. *Mining Science and Technology*, 2010, 20: 794–796.

[3] SU C J, ZHANG G H, ZHAO J. Researches of warm extrusion forming technology and property on 42CrMo steel cutting pick[J]. *Advanced Materials Research*, 2011, 337: 536–541.

[4] SU C J, LI Q L, XIAO L J, et al. Mechanical analysis of warm extrusion precision forming on 42CrMo steel cutting pick[J]. *Advanced Materials Research*, 2012, 538–541: 1061–1066.

[5] LI J N, LI H Q, WANG M, et al. Applications of WC-based composites rapid synthesized by consumable electrode in-situ

metallurgy to cutting pick[J]. *International Journal of Refractory Metals & Hard Materials*, 2012, 35: 132–137.

[6] LIU S Y, DU C L, CUI X X. Research on the cutting force of a pick[J]. *Mining Science and Technology*, 2009, 19(4): 514–517.

[7] LIU S Y, DU C L, CUI X X, et al. Cutting experiment of the picks with different conicity and carbidetip diameters[J]. *Journal of China Coal Society*, 2009, 34(9): 1276–1280. (in Chinese)

[8] SU O, AKCIN N A. Numerical simulation of rock cutting using the discrete element method[J]. *International Journal of Rock Mechanics & Mining Sciences*, 2011, 48: 434–442.

[9] REHBINDER G. Some aspects on the mechanics of erosion of rock with a high speed water jet[C]//*Third Intemational Simposium on Jet Cutting Technology*, Chicago, USA, E1, 1976.New York: Springer, 1976: 1–20.

[10] REHBINDER G. A theory about cutting rock with a water jet[J]. *Rock Mechanics*, 1980, (12): 247–257.

[11] TUTLUOGLU L. Mechanism of WARC[C]//*Proceedings of the* USA *Simposium on Rock Mechanism*, Chicago, USA, E3, 1983, New York: Springer, 1983: 202–210.

[12] LI X B, SUMMERS D A, RUPERT G, et al. Experimental investigation on the breakage of hard rock by the PDC cutters with combined action modes[J]. *Tunnelling and Underground Space Technology*, 2001, 16: 107–114.

[13] KOTWICA K. Results of laboratory investigations into operating conditions of cutting tool[J]. *Journal of Mining Science*, 2003, 39(2): 168–173.

[14] CICCU R, GROSSO B. Improvement of the excavation performance of PCD drag tools by water jet assistance[J]. *Rock Mechanics and Rock Engineering*, 2010, 43: 465–474.

[15] OZCELIK Y, TERCAN A E, CICCU R, et al. A Study of nozzle angle in stone surface treatment with water jets[J]. *Construction and Building Materials*, 2011, 25: 4271–4278.

[16] OZCELIK Y, CICCU R, COSTA G. Comparison of the water jet and some traditional stone surface treatment methods in different lithotypes[J]. *Construction and Building Materials*, 2011, 25: 678–687.

[17] OZCELIK Y, GURSEL M, CICCU R, et al. Optimization of working parameters of water jet cutting in terms of depth and width of cut[J]. *Proceedings of the Institution of Mechanical Engineers, Part E: Journal of Process Mechanical Engineering*, 2012, 226(1): 64–78.

[18] YANG X F, LI X H, LU Y Y. Wear characteristics of the cemented carbide blades in drilling limestone with water jet[J]. *International Journal of Refractory Metals & Hard Materials*, 2011, 29: 320–325.

[19] LU Y Y, TANG J R, GE Z L, et al. Hard rock drilling technique with abrasive water jet assistance[J]. *International Journal of Rock Mechanics & Mining Sciences*, 2013, 60: 47–56.

[20] PENG G Y, SHIMIZU S J. Progress in numerical simulation of cavitating water jets[J]. *Journal of Hydrodynamics,* 2013, 25(4): 502–509.

[21] DEHKHODA S, HOOD M. An experimental study of surface and sub-surface damage in pulsed water-jet breakage of rocks[J]. *International Journal of Rock Mechanics & Mining Sciences*, 2013, 63: 138–147.

[22] DEHKHODA S, HOOD M. The internal failure of rock samples subjected to pulsed water jet impacts[J]. *International Journal of Rock Mechanics & Mining Sciences*, 2014, 66: 91–96.

[23] GRYC R, HLAVÁČ L M, MIKOLÁŠ M, et al. Correlation of pure and abrasive water jet cutting of rocks[J]. *International Journal of Rock Mechanics & Mining Sciences*, 2014, 65: 149–152.

[24] AYDIN G. Recycling of abrasives in abrasive water jet cutting with different types of granite[J]. *Arabian Journal of Geosciences*, 2014, 15: 278–282.

[25] CICCU R, GROSSO B. Improvement of Disc cutter performance by water jet assistance[J]. *Rock Mechanics and Rock Engineering*, 2014, 47: 733–744.

[26] LIU S Y, LIU Z H, CUI X X, et al. Rock breaking of conical cutter with assistance of front and rear water jet[J]. *Tunnelling and Underground Space Technology*, 2014, 42: 78–86.

[27] LIU S Y, CHEN J F, LIU X H. Rock breaking by conical pick assisted with high pressure water jet[J]. *Advances in Mechanical Engineering*, 2014.

[28] SONG D Z, WANG E Y, LIU Z T, et al. Numerical simulation of rock-burst relief and prevention by water-jet cutting[J]. *International Journal of Rock Mechanics & Mining Sciences*, 2014, 70: 318–331.

[29] QU Q L, WU J L, GUO B D, et al. Numerical simulation of sphere impacting water by SPH with hydrodynamics[J]. *Advanced Materials Research*, 2013, 625: 104–108.

[30] LIAO H L, LI G S, NIU J L. Influential factors and mechanism analysis of rock breakage by ultra-high pressure water jet under submerged condition[J]. *Chinese Journal of Rock Mechanics and Engineering*, 2008, 27(6): 1243–1250. (in Chinese)

[31] MA G W, WANG X J, REN F. Numerical simulation of compressive failure of heterogeneous rock-like materials using SPH method[J]. *International Journal of Rock Mechanics and Mining Sciences*, 2011, 48(3): 353–363.

[32] WANG J M, GAO N, GONG W J. Abrasive water jet machining simulation by coupling smoothed particle hydrodynamics finite element method[J]. *Chinese Journal of Mechanical Engineering*, 2010, 23(5): 568–573.

[33] BUI H H, SAKO K, FUKAGAWA R. Numerical simulation of soil-water interaction using smoothed particle hydrodynamics (SPH) method[J]. *Journal of Terramechanics*, 2007, 44: 339–346.

[34] SONG Z C, CHEN J M, LIU F. Numerical simulation for high-pressure water jet breaking rock mechanism based on SPH algorithm[J]. *Oil Field Equipment*, 2009, 38(12): 39–43.

[35] YU T, TENG J G, WANG Y L, et al. Finite element modeling of confined concrete-I:Drucker–Prager type plasticity mode[J]. *Engineering Structures*, 2010, 32(3): 665–679.

Biographical notes

LIU Songyong, born in 1981, is currently a professor at *School of Mechatronic Engineering, China University of Mining and Technology, China*. He received his PhD degree from *China University of Mining and Technology, China*, in 2009. His research interests include the design and dynamics of excavation machinery, rock breaking assisted with water jet.
Tel: +86-13912033086; E-mail: lsycumt@163.com

LIU Xiaohui, born in 1988, is currently a PHD candidate at *School of Mechatronic Engineering, China University of Mining and Technology, China*. He received his bachelor degree from *China University of Mining and Technology, China*, in 2011. His research interests include the design and dynamics of excavation machinery, rock breaking assisted with water jet.
Tel: +86-15896421235; E-mail: TB13050011@163.com

CHEN Junfeng, born in 1989, is currently an engineer at *Research Institute of Zhejiang University, Taizhou, China*. He received his master degree from *China University of Mining and Technology, China*, in 2014. His research interests include the design and dynamics of excavation machinery, rock breaking assisted with water jet.
Tel:+86-15896421041; E-mail: chenjunfengcumt@163.com

LIN Mingxing, born in 1966, is currently a professor at *School of Mechanical Engineering, Shandong University, China*. He received his PhD degree from *China University of Mining and Technology, China*, in 1999. His research interests include machine vision detection, micro machining and manufacturing.
Tel:+86-13023613398; E-mail: linmx200@163.com